Impact of Receiver Deadtime on Photon-Counting SLR and Altimetry during Daylight Operations

John J. Degnan

Sigma Space Corporation

John.Degnan@sigmaspace.com /Fax: +01-301-577-9466

Abstract

The dominant noise source in photon-counting SLR and altimetry systems is the solar background during daylight operations. We discuss the relevant attributes of Single Photoelectron Avalanche Diodes (SPADs) and Microchannel Plate Photomultipliers (MCP/PMTs) for these applications. Using a solar noise model based on a stratified spherical shell atmosphere, we compute the expected background count rates under a variety of atmospheric conditions for two pertinent instruments, i.e. NASA's NGSLR (SLR2000) system and the Cross Track Channel Lidar Altimeter proposed for the ICESat-II Mission. We discus the relevant merits of the various detector types and the role various types of pre-detection noise filters can play.

Background Noise Sources for SLR and Laser Altimetry

Sources of background noise for SLR include detector dark counts, solar scattering off the atmosphere, and laser backscatter from instrument optics or the local atmosphere. In laser altimetry, one must also add solar scatter off the surface being interrogated.

Detector dark counts are spontaneous and random photon events that occur in a darkened environment without any apparent external stimulus. Dark count rates are generally lower in the visible wavelength regime and increase as one moves the operating wavelength deeper into the near infrared (NIR). Dark count rates can often be reduced by cooling the detector.

Solar photons enter the receiver by scattering off objects within the receiver Field-of-View (FOV) and are by far the dominant source of noise during daylight operations. In SLR, these photons are scattered by atmospheric constituents, such as molecules, aerosols, fog, clouds, etc. In altimetry, one has an additional, and usually dominant, solar contribution from the surface lying within the receiver FOV.

Another source of photon noise is laser backscatter off the instrument optics and/or nearby atmosphere. This is of special relevance to monostatic photon-counting systems, such as NASA's Next Generation Satellite Laser Ranging (NGSLR) station, when atmospheric scatter from the outgoing pulse falls within the temporal receive gate of a previous pulse. NGSLR periodically varies the laser pulse repetition rate slightly in an attempt to avoid this temporal overlap and has the additional option (not currently implemented operationally) of isolating the receiver from backscatter using a high speed, liquid crystal, optical gate [Degnan and Caplan, 2006]. Bistatic systems, whose transmit and receive FOV's are spatially isolated out to some range due to separate non-coaxial optical systems, are far less vulnerable to this type of backscatter noise.

Photon-Counting Detectors and Limitations

Kilohertz photon-counting SLR and altimetry systems employ either Single Photon Avalanche Photodiodes (SPADs) or MicroChannel Plate PhotoMultiplier Tubes (MCP/PMTs) as detectors. Both detector types have high quantum efficiencies (40% to 55%) at the 532 nm SLR wavelength. When used in the near infrared (NIR), commercially available Geiger-mode SPAD's and MCP/PMT's have traditionally been plagued by relatively low efficiencies (<4%) and high dark counts when compared to their visible counterparts. More recently, however, MIT Lincoln Laboratories has reported on passively-quenched NIR APD arrays with about 55% efficiency at 1064 nm. Similarly, Hamamatsu has recently introduced a cooled NIR MCP/PMT with QE's as high as 18% (10% is nominal).
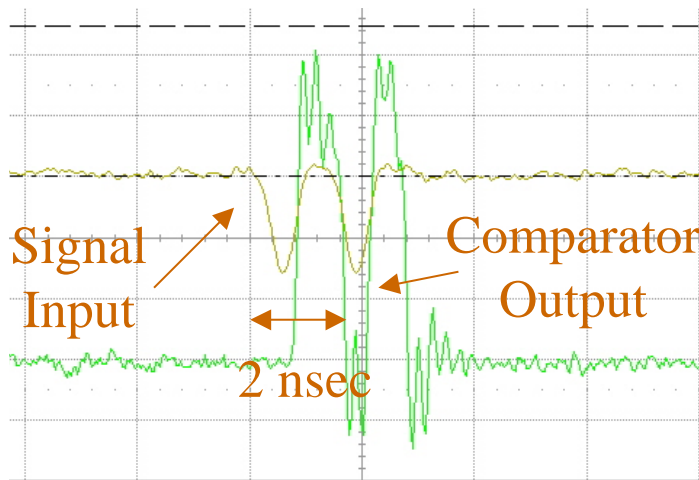
Figure 1. Sigma Space Corporation has built a 50 channel timing board with a timing precision of $\pm$ 93 psec ($\pm$1.4 cm) and a recovery time of about 1.6 nsec as part of a 100 beam, airborne 3D imaging lidar. The waveforms demonstrate the ability of the timing receiver to resolve input signals separated by only 2 nsec.

SPADs are further divided into passively or actively quenched subgroups with vastly different recovery times following a photon event. Passively-quenched SPADs (PQ-SPADs) have recovery times on the order of 1.6 microseconds, which essentially makes them "single-stop per pulse" devices for most lidar applications. Actively quenched SPADs (AQ-SPADs) , on the other hand, typically have recovery times on the order of 50 nsec. In contrast, MCP/PMTs have vanishingly small recovery times (< 2 nsec), but this inherent advantage is not always maintained by the backend timing electronics. In NASA's NGSLR system, for example, the HTSI-built timing electronics recovery time is comparable to that of an actively-quenched SPAD receiver, whereas the combined MCP/PMT detector and timing electronics in Sigma's 100 beam 3D Imaging Lidar [Degnan et al, 2007] has a much shorter recovery time, about 1.6 nsec. Fast recovery times also enhance the performance of laser altimeters measuring surface topography through semi-porous obscurations, such as tree canopies, ground fog, clouds, dust, etc.

Impact of Solar Noise on Photon-Counting Detectors

High solar background rates can reduce the probability of detecting the signal if the detector or receiver have recovery times, τ_d, comparable to or greater than the mean time between solar photon arrivals. In general, the solar photon count rate, $\dot{n}$, will cause the mean signal count rate from the satellite or the ground to be reduced by a factor

$$SCRF = \exp\left(-\dot{n}\,\tau_d\right) \tag{1}$$

which corresponds to the Poisson probability that a solar count will not be detected within a receiver deadtime interval prior to a signal "event". In Figure 2, we plot the "Signal Count Reduction Factor" (SCRF) as a function of solar background rate for the three photon-counting detectors discussed previously, i.e. the PQ-SPAD, AQ-SPAD, and MCP/PMT.
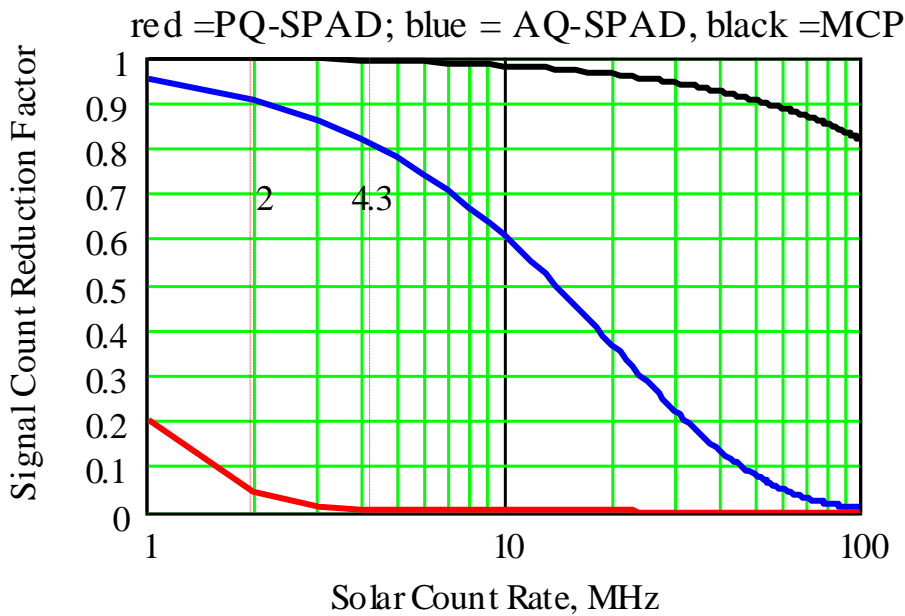
Figure 2. Signal count reduction factor vs solar count rate for three common photon-counting detectors: red = PQ- SPAD (1600 nsec), blue = AQ-SPAD (50 nsec), and black = MCP/PMT (2 nsec).

MCP/PMTs have one disadvantage relative to AQ-SPADs. High solar background rates can: (1) cause the microchannel plates to temporarily exceed their current limits (typically 100 to 200 nA) and reduce responsivity; and (2) reduce microchannel plate photomultiplier lifetime by extracting excessive charge from the microchannels. SPAD lifetimes do not appear to be limited by total charge extraction but rather by malfunctions in their associated electronics.

High solar background rates also reduce the *signal contrast* [Degnan, 2002a], analogous to Signal-to-Noise Ratio in multiphoton lidars, making the satellite or surface returns more difficult to identify against the background. Unless the noise can be successfully filtered pre-

detection or edited out via near real-time post-detection algorithms [Degnan, 2002a], ultralow contrast can add significantly to in situ data storage and transfer requirements.

Solar Noise Models for SLR and Altimetry

In performing the numerical studies presented here, we have employed a simple closed-form solar noise model, which assumes isotropic scattering in a stratified spherical shell atmosphere [Degnan, 2002b]. For photon-counting SLR systems, the solar count rate is given by

$$
\begin{aligned}
\dot{n} &= \frac{\eta_q \eta_r}{h\nu} \frac{N_\lambda (\Delta\lambda)\Omega_r A_r}{4\pi} \left\{ \sec\theta_t T_0^{\sec\theta_t} \left[\frac{1 - T_0^{\sec\theta_s - \sec\theta_t}}{\sec\theta_s - \sec\theta_t} \right] \right\} \\
&\cong \frac{\eta_q \eta_r}{h\nu} \frac{N_\lambda (\Delta\lambda)\Omega_r A_r}{4\pi} \left\{ T_0^{\sec\theta_t} \ln\left(\frac{1}{T_0^{\sec\theta_t}} \right) \right\}
\end{aligned}
\tag{2}
$$

where, for NGSLR, $\eta_q = 0.28$ is the MCP/PMT detector counting efficiency, $\eta_r = 0.4$ is the throughput efficiency of the receiver optics, $h\nu$ is the laser photon energy, N_λ is the exo-atmospheric spectral irradiance at the laser wavelength (0.2W/m^2-A^o-ster @ 532 nm), $\Delta\lambda = 3A^o$ is the FWHM bandwidth of the spectral filter, $A_r = 0.126\text{m}^2$ is the telescope receive area, Ω_r is the receiver solid angle, T_0 is the one-way atmospheric transmission at zenith, θ_s is the solar zenith angle, and θ_t is the target (satellite) zenith angle. The *atmospheric factor* in {brackets} is plotted for NASA's NGSLR System versus the satellite zenith angle in Figure 3. The four plots correspond to $T_0 = 0.8, 0.6, 0.4,$ and 0.2 and the curves within each plot correspond to different solar zenith angles. The black curve in each graph is a plot of the approximate expression in (2) which is generally valid for $T > 0.6$ and $\theta_t < 60^o$.

From Figure 3, one can conclude that an Atmospheric Factor (AF) = 0.5 is a "worst case" value for target zenith angles less than 70°. In Figure 4, we plot (2) for NGSLR with AF = 0.5 to obtain a worst case noise count as a function of the receiver half-angle FOV, ω, which is related to the receiver solid angle by $\Omega_r = \pi\omega^2$. Since the NGSLR timer has a 60 nsec deadtime (comparable to an actively-quenched SPAD), it will lose 10% or more of the target data for $\omega > 5.3$ arcsec.
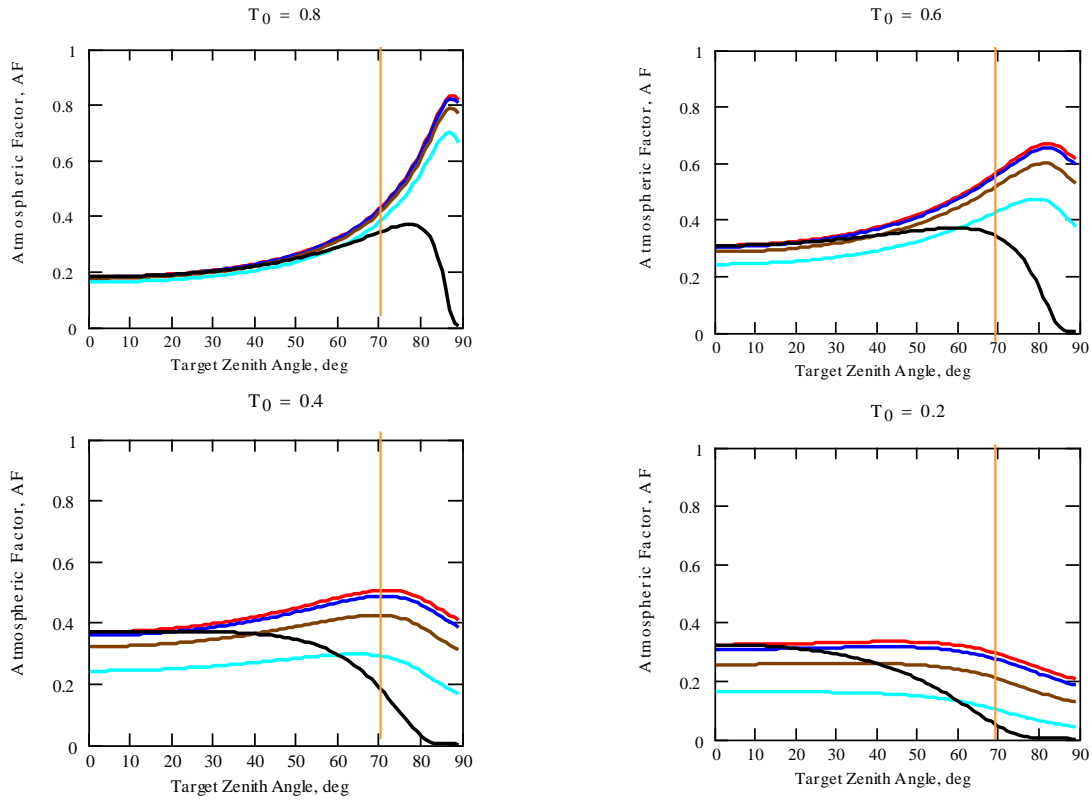
Figure 3. Plots of the atmospheric factor in (2) for NASA's NGSLR system vs target (satellite) zenith angle. The four graphs correspond to four different zenith atmospheric transmissions (T_0 = 0.8, 0.6, 0.4, and 0.2) while the curves within each figure correspond to different solar zenith angles in degrees, i.e. θ_s = 0 (red), 20 (blue), 40 (brown), and 60 (magenta). The black curves correspond to the approximate expression in (2) which is only valid for high transmissions (T_0 >0.6) and lower target zenith angles (θ_t <60°).
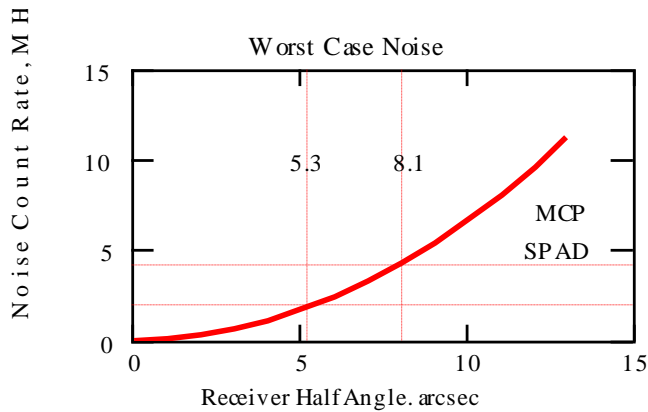
Figure 4. Solar noise count rate vs NGSLR receiver FOV half angle assuming a worst case atmospheric factor, AF =0.5. For a nominal half angle of 5.3 arcsec, approximately 10% of the satellite data will be lost due to the slow recovery time of the HTSI timing receiver, which negates the inherent recovery time advantage of NGSLR's MCP/PMT.

For laser altimetry, we have the following expression for the solar count rate due to the combined scattering off the surface and intervening atmosphere [Degnan, 2002a]

$$\dot{n} = \left[\frac{\eta_q \eta_r}{h\nu} \right] \left[\frac{N_\lambda^0(\Delta\lambda)\Omega_r A_r}{\pi} \right] \left[\rho T_0^{1+\sec\theta_s} \cos\psi + \frac{1 - T_0^{1+\sec\theta_s}}{4(1 + \sec\theta_s)} \right] \tag{3}$$

where ρ is the surface reflectance and ψ is the angle between the surface normal and the Sun. For this example, we consider the photon-counting, Cross Track Channel (CTC) Lidar proposed by Sigma to fly alongside the primary GLAS-II lidar on NASA's ICESat-II Mission and described elsewhere in these Proceedings [Degnan, 2008]. The CTC is designed to generate 16 parallel tracks of surface profile data as in Figure 5a. The plots in Figure 5b assume a nominally flat ($\psi \sim \theta_s$), high reflectance ($\rho = 0.94$), Lambertian ice/snow surface, and a receiver solid angle per channel of $\Omega_r = 2\times10^{-9}$ ster , corresponding to a 30 m diameter ground spot at 600 km altitude. As in ICESat-1, the green channels share the 1 m telescope ($A_r = 0.736$ m^2) with the primary 1064 nm lidar, and an additional 25 pm etalon filter in the receiver reduces the solar count rate by an additional factor of 10 relative to the 250 pm GLAS "coarse" spectral filter. The etalon extends tube life by a similar factor by reducing the overall charge transfer rate from photocathode to anode , but the transmission peak of the etalon filter must actively track the laser transmitter wavelength. Cloud cover is included in the atmospheric transmission T_0, which, in Figure 5b, is varied from 1.0 (no atmosphere) to 0 (thick clouds). In the latter case, neither the lidar nor solar rays can penetrate to the surface.

.

(a)   (b)
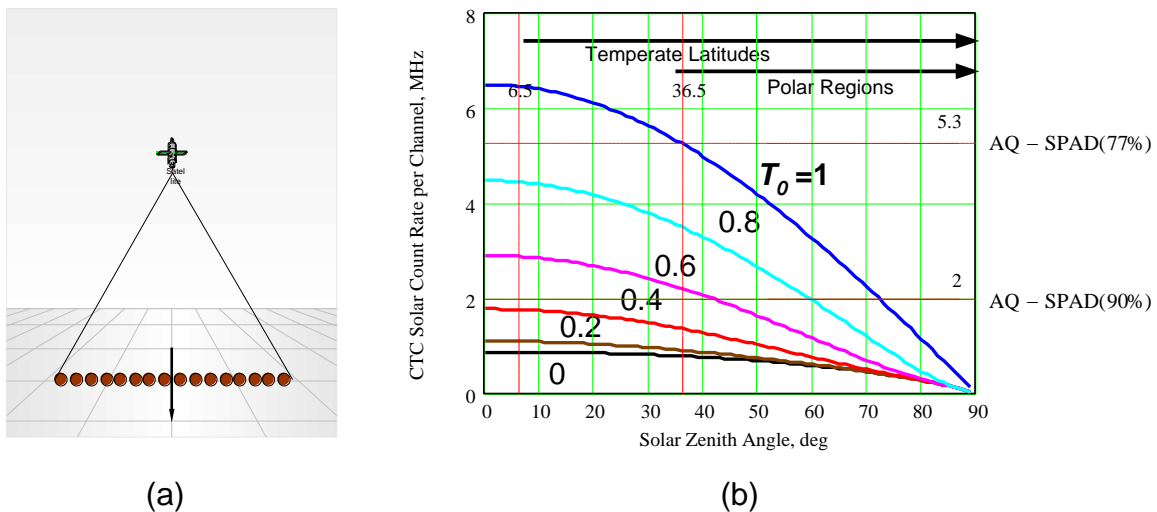
Figure 5. (a) CTC 16 beam lidar concept; (b) Solar background rate for a single CTC channel with the 25 pm GLAS etalon over a Lambertian ice/snow surface as a function of solar zenith angle and the one-way zenith atmospheric transmission, T_0. In the polar regions (LAT>60°), the minimum solar angle is 36.5°, and the SCRF is reduced to about 77% for the AQ-SPAD in extremely clear atmospheres.

The Role of Pre-Detection Filtering

There are four pre-detection filtering techniques that can be employed [Degnan, 1993]:
1. **Spectral** – choose narrowband filters trading off between bandwidth, optical throughput, and added operational complexity

2. **<u>Spatial</u>** – use minimum receive FOV consistent with transmitter divergence, telescope image quality, and transmit/receive co-boresight stability.
3. **<u>Temporal</u>** – use range gates to only accept returns from the region of interest and reject other regions.
4. **<u>Amplitude</u>** – choose receiver detection thresholds to eliminate background "false alarms" in high SNR systems.

As can be seen from (2) and (3), the solar count rate seen by the detector can only be reduced through the use of spectral ($\Delta\lambda$) and/or spatial (Ω_r) filtering.

Temporal filtering, or range gating, has no effect on the SCRF as defined by (1) unless the range gate can be set very narrow, i.e. to a small fraction of the mean time between solar counts. Temporal filtering can, however, lower the mean current in an MCP/PMT, preventing the MCP from reaching saturation, preserving responsivity, and extending MCP/PMT lifetime.

Since by definition photon-counting systems detect single photon events, amplitude filtering is not generally applicable except for eliminating low-level electronics noise. It was determined analytically that raising the detection threshold above 1 pe (amplitude filtering) for the CTC application resulted in a significant loss of surface data without providing commensurate noise reduction benefits.

Summary

The combined detector/receiver recovery time determines the maximum tolerable noise count rate in photon-counting lidars. During night operations, when the noise background is dominated by detector dark counts , Microchannel Plate Photomultipliers (MCP/PMTs) and Single Photon Avalanche Diodes (SPADs) are predicted to work equally well for "single stop applications", which include SLR, transponders, or altimetry over unobscured terrain. During daylight operations, however, the target return rate will be substantially reduced if the mean time between solar counts is not much greater than the recovery time of the overall receiver. The solar background count rate can only be managed by limiting the telescope aperture or optical throughput, spatial field-of-view, and/or spectral filter bandwidth. Temporal filtering (range gating) has no impact on recovery time limitations of SPAD's unless the gate can be set very narrow relative to the mean arrival time between solar photons, but gating can prevent microchannel plate saturation in an MCP/PMT, preserve responsivity, and significantly extend tube life. Gating also reduces data storage and/or transmission requirements, and aids the post-detection filtering process. It was determined that raising the detection threshold above 1 pe (amplitude filtering) results in a significant loss of target data without providing commensurate noise benefits. Photon-counting systems, such as NASA's NGSLR/SLR2000 station and a proposed multichannel spaceborne altimeter on ICESAt-II, the Cross Track Channel Lidar, were used as examples to illustrate these important effects.

References

Degnan, J., "Millimeter Accuracy Satellite Laser Ranging: A Review", in <u>Contributions of Space Geodesy to Geodynamics: Technology</u>, D. E. Smith and D. L. Turcotte (Eds.), AGU Geodynamics Series, Volume 25, pp. 133-162, 1993.

Degnan, J., "Photon-Counting Multikilohertz Microlaser Altimeters for Airborne and Spaceborne Topographic Measurements", Journal of Geodynamics, 34, pp. 503-549, November, 2002a,.

Degnan, J. "Asynchronous Laser Transponders for Precise Interplanetary Ranging and Time Transfer", Journal of Geodynamics , pp. 551-594, November, 2002b.

Degnan, J., Caplan, D. 2006, "Performance of a Liquid Crystal Optical Gate for Suppressing Laser Backscatter in Monostatic Kilohertz SLR Systems", Proc. 15th International Workshop on Laser Ranging, Canberra, Australia, October 16-20.

Degnan, J., Wells, D., Machan, R., Leventhal, E., "Second Generation 3D Imaging Lidars Based on Photon-Counting", SPIE Optics East , Boston, MA, September 9-12, 2007.

Degnan, J., 2008, "Globally Contiguous, High Resolution Topographic Mapping of Planets and Moons via Photon-Counting", these Proceedings.